A C-Band Intermodulation Radar System for Target Motion Discrimination

Ashish Mishra, Changzhi Li Department of Electrical Engineering, Texas Tech University, Lubbock, TX USA 79409

Abstract — This paper discusses the design and test of an intermodulation radar receiver and a nonlinear tag. To discriminate reflections at the fundamental and the third-order intermodulation frequencies, the receiver was designed to attenuate the fundamental reflections and amplify the lower 3rd-order tone generated by the nonlinear target. The nonlinear tag was designed on a flexible substrate for wearable applications. Experiments were performed with two types of targets, i.e., the nonlinear tag and a metal reflector. The results were recorded and analyzed to demonstrate the clutter noise rejection capability of the intermodulation radar.

Index Terms— clutter rejection, intermodulation, nonlinear tag, nonlinear radar.

I. INTRODUCTION

Non-linear radars are used to track targets of interest and reject clutters. These radars identify the nonlinear characteristics present in many electronic components, such as diodes and transistors. Since naturally occurring things are linear in behavior, they can be distinguished from the nonlinear components, which are man-made. In nonlinear radars, fundamental tone(s) is sent towards a nonlinear tag, which in return reflects nonlinear tone(s) along with the fundamental tone(s). In the receivers, the fundamental tone(s) is separated from nonlinear response to distinguish between targets and clutters [1-3].

Many nonlinear radars detect harmonics of the transmitted tone(s), which lead to some major challenges in design, e.g., radio spectrum licensing issues [3] [4] and high path loss of the harmonic tones compared with the fundamental tone(s). Since conventional filters can hardly meet the high-quality factor requirement, diplexers were used, making the system bulky and expensive. Since harmonic frequency tones occupy a bandwidth at least twice of the fundamental tones, many harmonic radars need to be very broadband.

Another commonly used nonlinear radar is subharmonic [5], here the fundamental response from the radar f is captured by the tag, and nonlinear response f/n, is reflected along with the fundamental. Here n, denotes the order of the subharmonic response. In these radars, the nonlinear responses have lower path loss at the cost of the larger receiver and tag size.

Recently, a new nonlinear response based on intermodulation response for target localization and clutter rejection purpose has been discussed [6,7]. In these nonlinear radars, the two fundamental tones are sent out towards the tag/nonlinear target; the tag absorbs these fundamental tones and reflects a series of intermodulation and harmonic responses. The receiver of these radars' separate 3rd order harmonic response and attenuate other responses. To achieve high rejection, diplexers were generally utilized. This leads to bulky and expensive radar systems.

In this paper, an intermodulation-based nonlinear radar is discussed to separate clutters from the target of interest. Here, diplexers were replaced with a series of gain blocks and filters to achieve comparable rejection for separating the target from the clutter. The receiver part of the radar is designed on a printed circuit board (PCB) with a 50-dB attenuation to fundamental tones and a 20-dB gain to the lower 3rd-order tone. This intermodulation radar can overcome some drawbacks of harmonic radars. Its 3rd-order tones are close to the fundamental tones, sharing almost the same path loss as the fundamental tones. Compared with the harmonic radar, which requires its nonlinear target to operate in two largely separated frequency bands, the intermodulation radar only needs a nonlinear target with a simple matching circuit to work in a single band and avoids licensing issues [8]-[10].

This paper is divided into four sections. Section II discusses the theory and design of the intermodulation radar and passive nonlinear tag. Section III presents the measurement results demonstrating motion discrimination. A conclusion is drawn in Section IV.

II. INTERMODULATION THEORY AND RECEIVER DESIGN

When two frequency tones f_1 and f_2 ($f_1 < f_2$) pass through a nonlinear device; additional frequency tones are generated at $mf_1 \pm nf_2$, where m and n could be any integer numbers. The lower $3^{\rm rd}$ -order tone $f_{r1} = 2f_1 - f_2$ is used in this radar as they are close to fundamentals. The receiver is designed to attenuate frequencies above $f_{r2} = 2f_1 - f_2$.

A. Radar system

Figure 1 shows the complete block diagram of the intermodulation radar. To maintain coherence and achieve required sensitivity based on the range correlation effect [11], all the three signal generators are tied to the same reference, which was provided by signal generator SG3. Two fundamental tones of equal amplitudes were generated using SG1 and SG2, and fed to the transmitting antenna through the power combiner. The two transmitted tones are denoted as:

$$T(t) = \sum_{i=1}^{2} \cos[2\pi f_i t + \phi(t)]$$
 (1)

where $\phi(t)$ is the phase noise of the two signal generators. The transmitted signal is sent to the target at a distance x_0 .

The nonlinear tag used in this project is passive and has Schottky diodes to generate nonlinear responses. As a result, the radar received signal can be expressed as:

$$R(t) = \cos\left[2\pi f_{r1}t - \frac{4\pi x_o}{\lambda} - \frac{4\pi x(t)}{\lambda} - \phi\left(t - \frac{2x_o}{c}\right)\right] \quad (2)$$

where λ is the wavelength corresponding to f_{r1} , x(t) is the mechanical displacement of the target, and the signal amplitude is normalized to 1. The fundamental components,

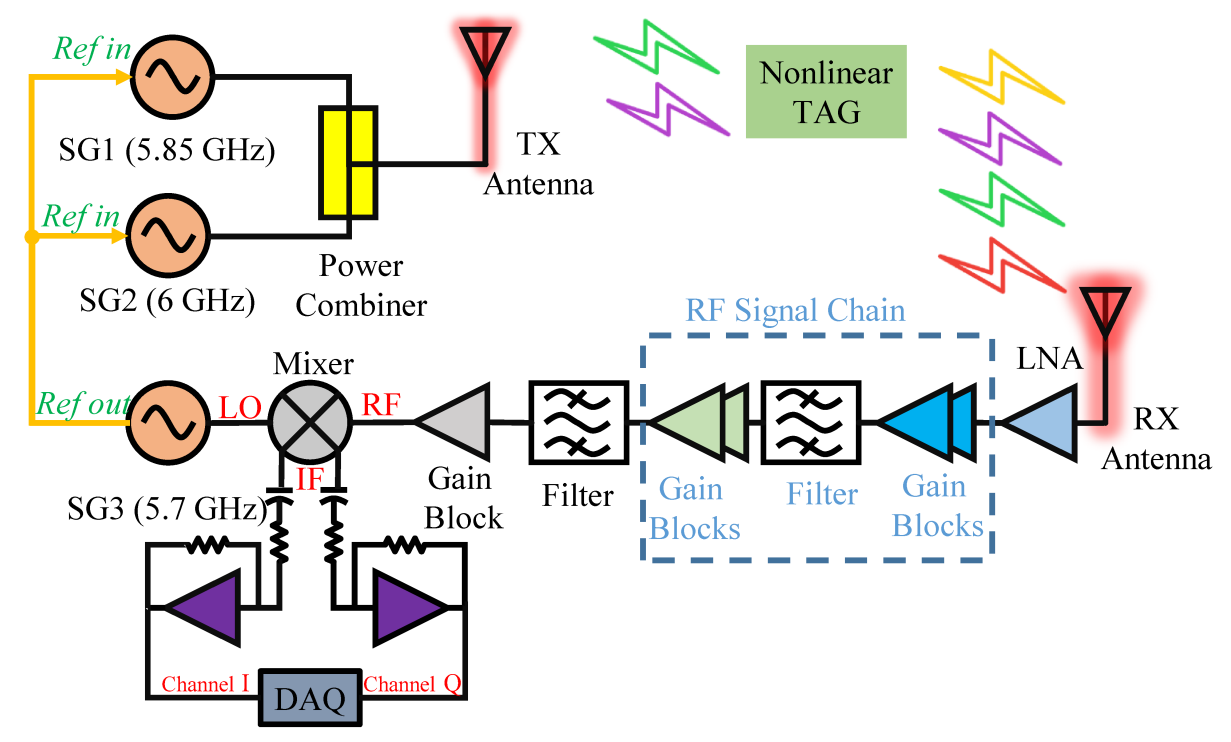


Fig. 1. The C-band intermodulation radar and its non-linear target.

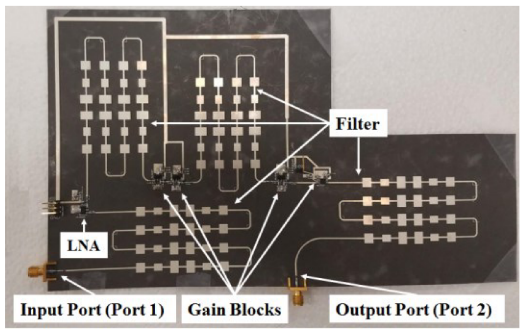


Fig. 2. The receiver RF signal chain of the intermodulation radar.

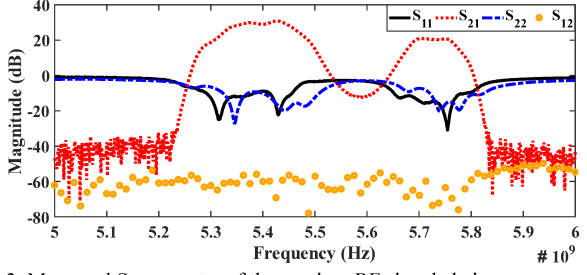


Fig. 3. Measured S-parameter of the receiver RF signal chain.

the higher $3^{\rm rd}$ -order component f_{r2} , and the other nonlinear tones are ignored in (2) as they will be at least 50-dB weaker than the f_{r1} tone at the input of the low noise amplifier (LNA) in the radar receiver. The LO port of the mixer is driven by a signal with frequency f_{r1} , which also provides additional rejection of other frequency tones.

The radar is AC-coupled at the mixer output to remove the DC offset, and the I and Q signals from the baseband amplifier can be expressed as:

$$B_{I/Q}(t) = A_{I/Q} \cos \left[\theta + \frac{4\pi x(t)}{\lambda} + \Delta \phi(t)\right]$$
 (3)

where $\theta = \frac{4\pi x_o}{\lambda} + \theta_o$ and θ_o accounts for the phase shift when the signal is reflected from the tag and propagates along

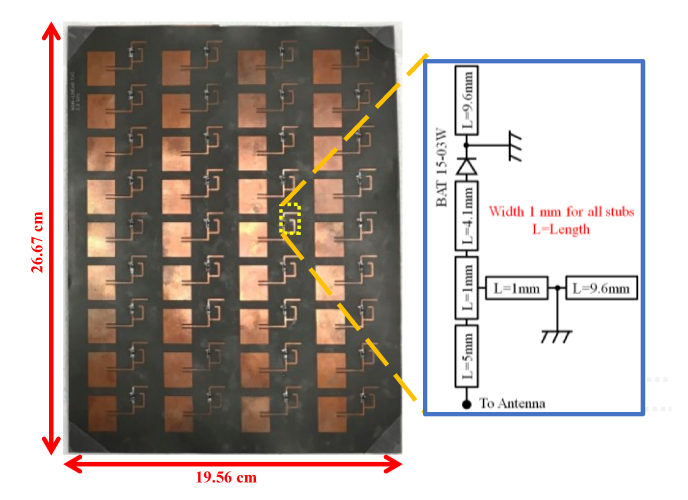


Fig. 4. Fabricated nonlinear tag with a unit shown in the inset.

building blocks in the radar signal chain. $\Delta \phi(t)$ is the residual phase noise, which can be ignored for short-range detection due to the range correlation effect [7]. A_I and A_Q are the amplitudes of the I/Q channel baseband outputs. The use of I/Q channels solves the null detection point issue [7]. These baseband signals are converted from analog to digital using NI-USB 6009 (DAQ).

B. Receiver RF signal chain

The receiver was designed with $f_1 = 5.85$ GHz and $f_2 = 6$ GHz. A combination of filters and amplifiers is used to attenuate the fundamental tones and amplify the lower $3^{\rm rd}$ -order tone. One of the key challenges of cascading amplifiers and filters is system stability. The receiver chain was finalized by performing system-level simulations in NI-AWR. The fabricated receiver RF signal chain is shown in Fig. 2.

The RF signal chain attenuates the fundamentals at 5.85

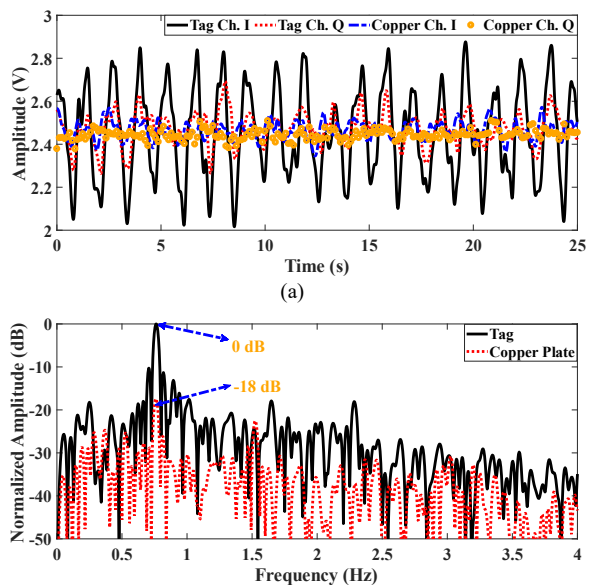


Fig. 5. A. Nonlinear tag vs. metal plate: (a) Baseband output for metal and nonlinear tag motion (b) FFT of baseband signal.

GHz and 6 GHz by 50 dB and provides 20.72-dB gain at 5.7 GHz. To achieve this, a 9th-order Chebyshev filter was designed to attenuate the tones at f_1 , f_2 and f_{r2} . The filter was designed and simulated with NI-AWR for RT/Duroid 5880 material. The filter provides over 40-dB attenuation to the fundamental tones.

Apart from attenuating the fundamental tone(s), the isolation is also a key criterion for the receiver design because the leakage from the local oscillator (LO) port to the radio frequency (RF) port can radiate back to the surrounding. Because of that, the corresponding clutter reflection can be comparable to the 3rd-order tone generated by the tag, leading to clutter interference. In this work, the reverse isolation from port 2 to port 1 is above 50-dB across the 5 to 6 GHz band.

C. Nonlinear tag

The passive nonlinear tag was designed for operation without requiring any battery. Figure 4 shows the nonlinear tag fabricated on RT/Duroid 5880 substrate and the schematic of its unit cell with the Infineon BAT 15-03W Schottky diode. The S-parameter model of the diode with 0-V and 0-mA bias was used to design the microstrip line matching circuit for each unit cell. A C-band patch antenna is also integrated into each unit cell. The tag contains a 4×9 array of unit cells.

III. EXPERIMENT

Two types of targets were used in the experiments, i.e., the fabricated nonlinear tag with a size of 26.67 cm×19.56 cm as shown in Fig. 4, and a copper plate with a size of 30.48 cm×22.86 cm. The copper plate was used to mimic an undesired clutter with a size larger than the nonlinear tag. A computer-controlled actuator and a motion phantom were used to generate mechanical movements. The actuator can generate an arbitrary movement amplitude and frequency. At the same time, the phantom is a battery-powered device with a rotating oval disc that generates a complex motion mimicking human breathing. All the measurements were recorded with the targets placed at 0.5-m away from the intermodulation radar.

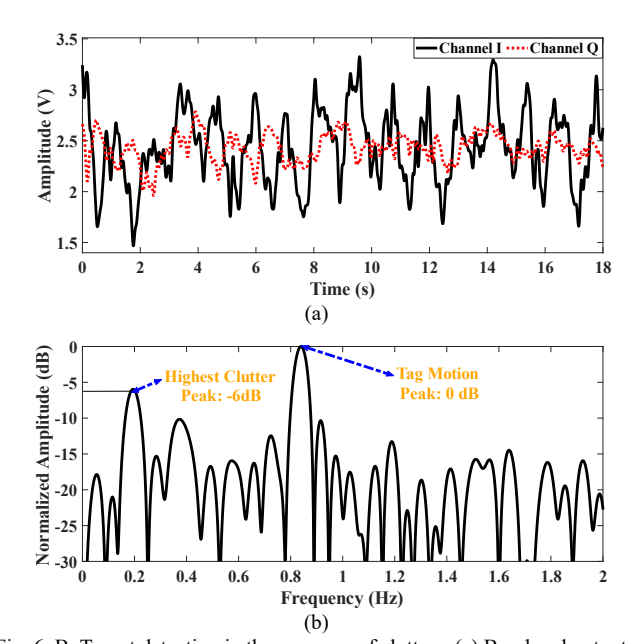


Fig. 6. B. Target detection in the presence of clutters: (a) Baseband output for metal and nonlinear tag motion (b) FFT of baseband signal.

A. Nonlinear tag vs. copper plate

In this measurement, the nonlinear tag and the copper plate were mounted sequentially on the actuator moving with 1-mm peak-to-peak amplitude and 0.8-Hz frequency in front of the radar. The baseband data was recorded, and Fast Fourier Transform (FFT) was performed. The results are shown in Fig. 5. From this graph, it can be seen that the signal detected from the nonlinear tag was 18-dB stronger than that detected from the copper plate, although the copper plate has a larger physical size than the nonlinear tag. The weak motion signal visible for the copper plate was mainly due to the nonlinearity of the amplifiers and mixer in the receiver chain.

B. Target detection in the presence of clutters

The second experiment demonstrated motion discriminating when a small motion of the nonlinear tag and a large motion of the copper plate coexist. In this case, the copper plate was placed on the motion phantom, which moved with approximately 10-mm peak-to-peak amplitude and a frequency of 0.2 Hz, while the nonlinear tag was placed on the actuator moving with a 2-mm peak-to-peak amplitude and 0.9-Hz frequency. The two objects were placed side by side in front of the radar.

Figure 6 shows the baseband signal detected by the radar and its corresponding spectrum. Although the copper plate has a larger size and moves with an amplitude five times higher than the nonlinear tag, the radar successfully detected the 0.9-Hz nonlinear tag motion. The radar also suppressed the 0.2-Hz strong clutter motion to 6-dB below the desired signal level.

IV. CONCLUSION

An intermodulation radar was designed and experimentally tested with different targets. The receiver board was able to amplify the 3rd-order frequency tone and attenuate the fundamental tones. The radar can successfully differentiate between the motions of a nonlinear tag from a large clutter. Compared to harmonic radars, the proposed intermodulation

radar operates in the same frequency band to transmit and receive signals, which simplifies the hardware design and avoids licensing issues due to multiple-band operation.

ACKNOWLEDGMENT

The authors would like to acknowledge grant support from National Science Foundation (NSF) ECCS-2030094 and ECCS-1808613.

REFERENCES

- [1] C. Mandel, C. Schuster, B. Kubina, M. Schüßler and R. Jakoby, "Dual Frequency Selective Multiple Access With Quasi-Chipless/Powerless RFID Mixer Tags," *IEEE Microw. Wireless Compon. Lett.*, vol. 24, no. 8, pp. 572-574, Aug. 2014.
- [2] Ashish Mishra and Changzhi Li "A third-order harmonic radar design for mm-wave frequencies", Proc. SPIE 11742, Radar Sensor Technology XXV, 117421A (12 April 2021)
- [3] Z. Tsai et al., "A High-Range-Accuracy and High-Sensitivity Harmonic Radar Using Pulse Pseudorandom Code for Bee Searching," *IEEE Trans. Microw. Theory Techn.*, vol. 61, no. 1, pp. 666-675, Jan. 2013.
- [4] Z. Peng, D. Psychogiou and C. Li, "Investigation of the roles of filters for a harmonic FMCW radar," *Int. Appl. Comput. Electromag. Soc.* (ACES) Symp., pp. 1-2, Suzhou, Aug. 2017.
- [5] N. El Agroudy, M. El-Shennawy, N. Joram and F. Ellinger, "Design of a 24 GHz FMCW radar system based on sub-harmonic generation", IET Radar Sonar Navigat., vol. 12, no. 9, pp. 1052-1057, Sep. 2018.
- [6] A. Mishra, W. McDonnell, J. Wang, D. Rodriguez and C. Li, "Intermodulation-Based Nonlinear Smart Health Sensing of Human Vital Signs and Location," in IEEE Access, vol. 7, pp. 158284-158295, 2019, doi: 10.1109/ACCESS.2019.2950347.
- [7] A. Mishra and C. Li, "A Low Power 5.8-GHz ISM-Band Intermodulation Radar System for Target Motion Discrimination," in IEEE Sensors Journal, vol. 19, no. 20, pp. 9206-9214, 15 Oct.15, 2019, doi: 10.1109/JSEN.2019.2926189.
- [8] A. Mishra, J. Wang, D. Rodriguez and C. Li, "Utilizing Passive Intermodulation Response of Frequency-Modulated Continuous-Wave Signal for Target Identification and Mapping," in IEEE Sensors Journal, vol. 21, no. 16, pp. 17817-17826, 15 Aug.15, 2021, doi: 10.1109/JSEN.2021.3084205.
- [9] A. Mishra and C. Li, "5.8-GHz ISM band intermodulation radar for high-sensitivity motion-sensing applications," 2018 IEEE Radio and Wireless Symp., pp. 4-6, Jan. 2018.
- [10] N. C. Kuo, B. Zhao and A. M. Niknejad, "A 10-Mb/s Uplink Utilizing Rectifier Third-Order Intermodulation in a Miniature CMOS Tag," *IEEE Microw. Wireless Compon. Lett.*, vol. 27, no. 11, pp. 1031-1033, Nov. 2017.
- [11] A. D. Droitcour, O. Boric-Lubecke, V. M. Lubecke, J. Lin and G. T. A. Kovacs, "Range correlation and I/Q performance benefits in singlechip silicon Doppler radars for noncontact cardiopulmonary monitoring," *IEEE Trans. Microw. Theory Techn.*, vol. 52, no. 3, pp. 838-848. March 2004.